Mixed Alkali Effect in Glasses

Jan Swenson[1] and Stefan Adams[2]

[1]*Department of Applied Physics, Chalmers University of Technology, S-412 96 Göteborg, Sweden*
[2]*GZG, Abteilung Kristallographie, Universität Göttingen, Goldschmidtstraße 1, D-37077 Göttingen, Germany*

(Received 29 October 2002; published 17 April 2003)

We have applied the bond-valence technique to reverse Monte Carlo produced structural models of mixed alkali phosphate glasses in order to elucidate the mixed alkali effect (MAE) in glasses. For the first time, the MAE is reproduced and understood directly from structural models in quantitative agreement with available experimental results. The two types of alkali ions are randomly mixed and have distinctly different conduction pathways of low dimensionality. This implies that *A* ions tend to block the pathways for the *B* ions and vice versa, and this is the main reason for the MAE.

DOI: 10.1103/PhysRevLett.90.155507 PACS numbers: 61.43.Fs

Solids with high ionic conductivity presently attract considerable scientific interest because of their potential applications as solid electrolytes in electrochemical devices such as batteries, chemical sensors, and "smart windows" [1]. The remarkable property of superionic solids is the selective ionic mobility in an otherwise nearly frozen material. However, it is well known that a high ionic conductivity can be ruined simply by substituting a fraction of the mobile ions by another type of mobile ions. This drop in conductivity is most pronounced for glasses and crystalline materials containing alkali ions and is therefore generally referred to as the mixed alkali effect (MAE) [2–4]. The MAE in glasses gives rise to large changes in many dynamic properties, particularly those related to ionic transport, when a fraction of the mobile ions is substituted by another type of mobile ions. Macroscopic properties such as molar volume and density, refractive index, thermal expansion coefficient, and elastic moduli usually change linearly or only slowly with composition. Properties related to structural relaxation, such as viscosity and glass transition temperature, usually exhibit similar deviations from linearity as other mixed glass-forming systems which do not contain any cations.

The peculiar MAE is only poorly understood, mainly due to the difficulty to determine the conduction pathways for the mobile ions. However, using reverse Monte Carlo [5,6] (RMC) produced structural models of mixed alkali phosphate glasses in combination with the bond-valence technique [7–9], we are able to determine the conduction pathways and to predict the experimentally observed MAE directly from the structural models.

Since the drop in conductivity (compared to the corresponding single alkali glasses) for an intermediate composition tends to increase with increasing size difference between the two types of alkali ions, we have chosen to study the glass system $Li_xRb_{1-x}PO_3$ ($x = 0$, 0.25, 0.5, 0.75, and 1), which can be considered as an archetypal glass system for investigations of the MAE. Figure 1 shows how the ionic conductivities of the single alkali glasses decrease by 6–8 orders of magnitude at the intermediate compositions ($x = 0.5$). This dramatic drop in conductivity cannot be explained by any major structural alteration upon the mixing of alkali ions. Rather, experimental results show [10–13] that the alkali ions tend to preserve their local structural environment regardless of the glass composition. Furthermore, the two types of alkali ions are randomly mixed in the glass [13–15]. Similar conclusions have been drawn from computer simulations of mixed alkali glasses [16–18]. Based on the experimental findings, a few theoretical models of the MAE have also been developed [19–22]. However, these models are in general also based on different more or less unverified assumptions, such as site relaxation, a selective hopping mechanism, or a crucial role of Coulomb interactions between the mobile ions, in contrast to our approach where the MAE is reproduced for structural models in quantitative agreement (as excellent as shown in Fig. 1 of Ref. [13]) with both neutron and x-ray diffraction data taken at the diffractometers LAD,

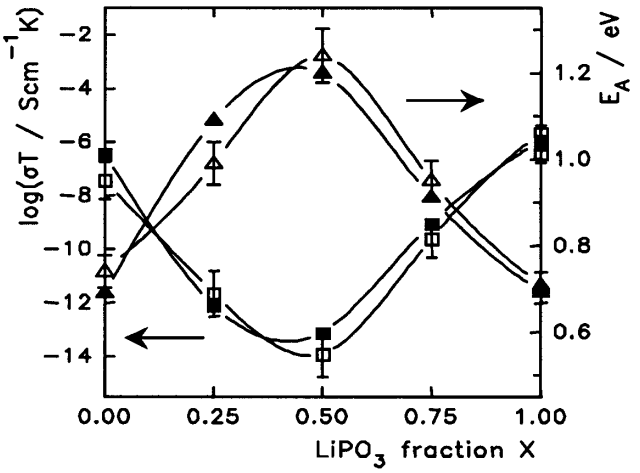

FIG. 1. Activation energy E_σ and dc conductivity σ_{dc} versus composition for the glass system $Li_xRb_{1-x}PO_3$ at 300 K. Open squares are experimental data points, taken from Ref. [29], and filled squares correspond to the values predicted from the pathway volume fractions F of the structural models. The solid lines are a guide to the eye.

Rutherford Appleton Laboratory, United Kingdom, and GILDA, European Synchrotron Radiation Facility (ESRF), Grenoble, France. The experimental procedure and data corrections were performed with great care and described in detail elsewhere [12,13].

In order to ensure that the RMC method [5,6] produces physically and chemically realistic structures of the metaphosphate glasses (e.g., that they consist of PO_4 tetrahedra sharing two corners and thereby forming polymerlike chains), the same bonding constraints were used as described in Ref. [13]. For each alkali ion, we ensured that realistic bonding distances and coordination number were obtained by using soft bond-valence constraints (described below) to minimize the deviation from the expected valence sum.

The bond-valence method is widely used in crystallography to evaluate the plausibility of proposed crystal structures [7–9]. It is based on the idea that the total bond-valence sum V of a M^+ ion may be expressed as

$$V = \sum_X s_{M^+-X}, \tag{1}$$

where the individual bond valences s_{M^+-X} for bonds to all adjacent anions X are commonly given by

$$s_{M^+-X} = \exp\left[\frac{R_0 - R_{M^+-X}}{b}\right]. \tag{2}$$

The bond-valence parameters R_0 and b are deduced from crystalline alkali oxide compounds with 96 different Li environments and 44 Rb environments. In all these different environments and coordination types, the monovalent alkali ions should have a bond-valence sum close to $V_{\text{ideal}} = 1$. Least squares refinements yielded $R_0 = 1.1745$ Å, $b = 0.514$ Å for Li-O, and $R_0 = 2.0812$ Å, $b = 0.415$ Å for Rb-O [23]. As for the crystalline compounds, the ion transport process from one equilibrium site to another should then follow the route which requires the lowest valence mismatch $\Delta V = |V - V_{\text{ideal}}|$, corresponding to the energetically most favorable pathway. Thus, in principle, the activation energy E_σ should be directly related to ΔV. However, since our structural models are of a relatively small size and ΔV shows large variations in the structure, it is not an easy task to determine the absolutely lowest value corresponding to the experimentally measured E_σ. A better way to quantify E_σ has shown to be to determine the pathway volume for a given value of ΔV [24]. For this purpose, the RMC produced structural models were divided into about 4×10^6 cubic volume elements [with a size of ca. $(0.2\ \text{Å})^3$], and ΔV was calculated for a hypothetical alkali ion (Li or Rb depending on the glass composition) at each volume element. The volume elements are classified as "accessible" for an alkali ion if $\Delta V < 0.2$ for that particular type of alkali ion or if V- V_{ideal} changes its sign across the volume element. The second criterion is needed to cushion the influence of our limited grid resolution. Accessible volume elements that share common faces or edges belong to the same "pathway cluster." If such a pathway cluster percolates through the structural model, it is considered to contribute to the dc conductivity. The relative volume of these percolating pathway clusters (in relation to the total volume of the system) is given by the pathway volume fraction F.

In Ref. [25], we have shown how the experimentally determined E_σ, as well as the dc conductivity σ_{dc}, are directly related to the cube root of the so obtained pathway volume fraction F multiplied by the square root of the mobile cation mass M. This relation holds for the present glasses, as well as for all the other ion conducting glasses we have tested, for any maximum value of ΔV as long as it is reasonably realistic ($\Delta V = 0.2$ valence units were used in this study). Thus, we are able to predict the values of E_σ and σ_{dc} directly from structural models and compare with the experimental values, as shown in Fig. 1. Considering the relatively large experimental errors (particularly in E_σ) for the glass compositions exhibiting the lowest conductivities, the agreement is fully satisfactory.

Figure 2 shows the RMC produced configuration of the $Li_{0.5}Rb_{0.5}PO_3$ glass. From the figure it is evident that the two types of alkali ions are randomly mixed, but not randomly distributed. Rather, the ions seem to be located in thin channels (which coincide with the low dimensional conduction pathways, shown in Fig. 3) running between the phosphate chains. Thus, the structure appears to be consistent with Greaves modified random network structure model [26].

In Figs. 3(a)–3(e), we show slices through the Li- and Rb-conduction pathways for all the investigated compositions of the $Li_xRb_{1-x}PO_3$ glass system. A few

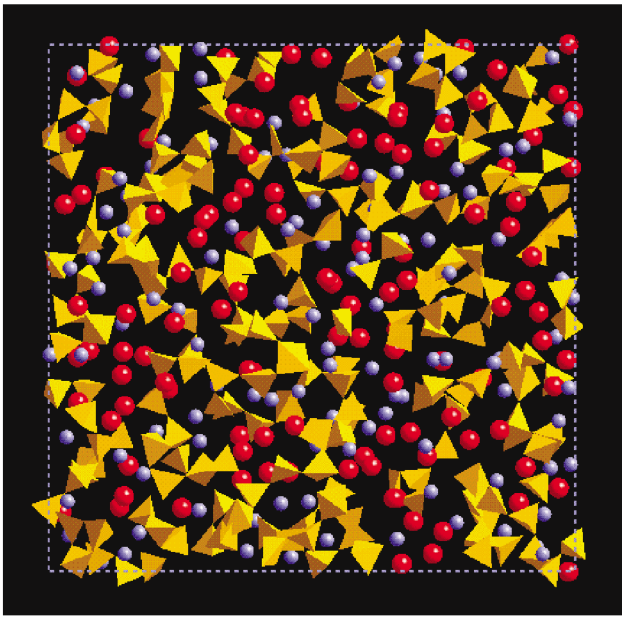

FIG. 2 (color). A 12 Å thick slice of the RMC produced structural model of the $Li_{0.5}Rb_{0.5}PO_3$ glass, respectively. Small blue spheres refer to Li, large red ones to Rb, and the PO_4 groups are shown as orange tetrahedra.

interesting points emerge directly from the pictures: (i) The pathway network is more extended for the $LiPO_3$ glass than for $RbPO_3$, explaining the higher conductivity of the former glass. (ii) For $Li_{0.5}Rb_{0.5}PO_3$, the pathway volume for the Li ions is considerably larger than for the Rb ions, which implies that Rb conduction gives only a minor contribution to the total conductivity. (iii) For all the mixed alkali glasses, Li and Rb ions have distinctly different conduction pathways.

Turning to Fig. 3(f), which again shows the Li pathways in $Li_{0.5}Rb_{0.5}PO_3$ plus those regions that are blocked by Rb ions but otherwise would have been conduction pathways for the Li ions, we can add a further point: (iv) The pathways for the Li ions are partly or totally blocked by Rb-rich regions and vice versa.

This blocking is highly effective due to the low dimensionality of the pathways, which becomes evident from Fig. 4. The figure shows for the $LiPO_3$ glass the number of sites at a distance up to r from a site in the infinite pathway cluster that are part of the same cluster. The slope of the log-log diagram represents the fractal dimension of the infinite pathway cluster, and is shown in the inset of Fig. 4 as a function of the chosen bond-valence mismatch threshold ΔV. As expected, the fractal dimension of the conduction pathways depends slightly on ΔV, but as long as the value is reasonably realistic (in relation to E_σ for this particular glass), we find a fractal dimension of around 1.8. Thus, we can conclude with the statement that the dimensionality of the conduction pathways is in the range 1.5–2.

Since the local structural environments of, for instance, Li and Rb ions are distinctly different, there is a large energy mismatch for Li jumps to Rb sites and vice versa [16,17]. This fact in combination with the low dimensionality of the pathways and the nonstatistic distribution of the cations (see Fig. 2) causes the strong blocking effect in the mixed alkali glasses. This reduces the possibility for, e.g., the Li ions to perform energetically favorable ionic jumps, giving an on average higher activation energy and a lower ionic conductivity. Thus, our approach shows that the MAE is a natural consequence whenever the mobile ions have different sizes and/or different polarizabilities/bond softnesses.

The fact that the MAE can be reproduced and understood from static structural models (i.e., without including any kind of structural relaxation, except the hopping motion of the alkali ions) further implies that the MAE had been too weak if we had allowed the local structure to relax on a time scale similar to the inverse hopping rate of the alkali ions. Thus, at room temperature such site

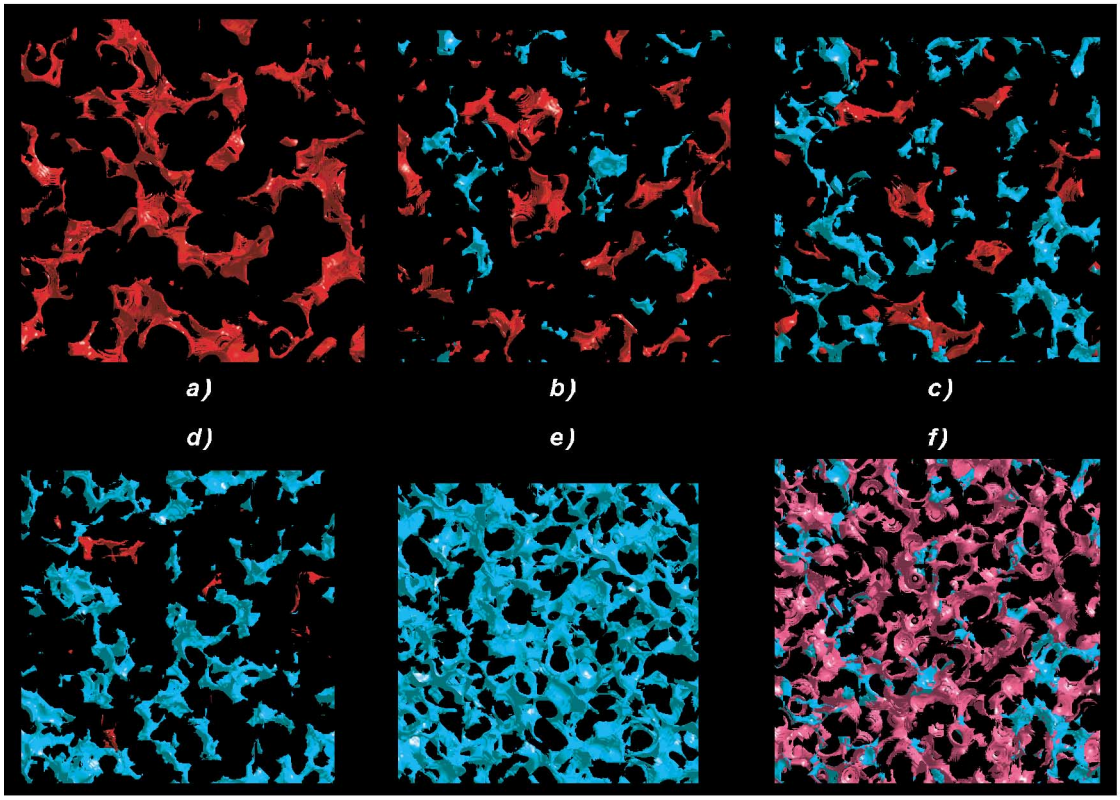

FIG. 3 (color). 7 Å thick slices through the conduction pathways ($\Delta V < 0.2$) for Li and Rb ions in the glasses $Li_xRb_{1-x}PO_3$: (a) $x = 0$; (b) $x = 0.25$; (c) $x = 0.5$; (d) $x = 0.75$; (e) $x = 1$. The pathways for the Li and Rb ions are shown as blue and red isosurfaces, respectively. (f) Li pathways in $Li_{0.5}Rb_{0.5}PO_3$ (blue) and those regions that are blocked by Rb ions but otherwise would have a matching bond valence and therefore been conduction pathways for the Li ions (pink).

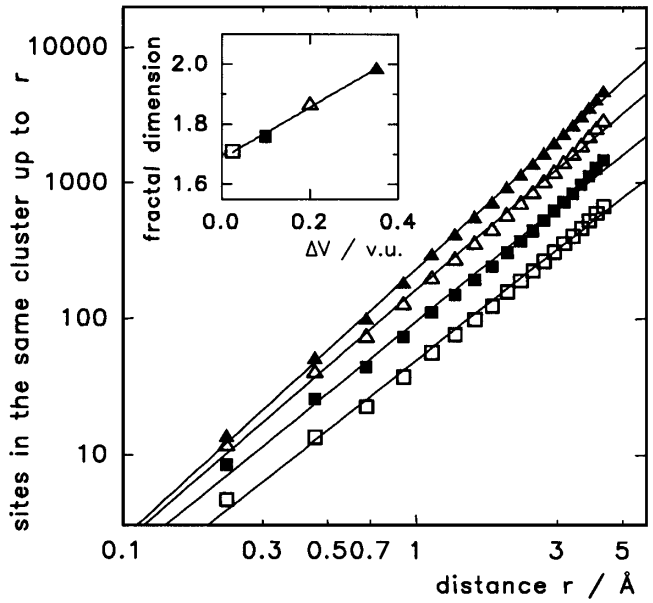

FIG. 4. Number of sites at a distance up to r from a site in the infinite pathway cluster that are also part of the same cluster, shown for the $LiPO_3$ glass for the valence mismatch threshold values $\Delta V = 0.025$ (open squares), $\Delta V = 0.1$ (filled squares), $\Delta V = 0.2$ (open triangles), and $\Delta V = 0.35$ (filled triangles). The slope of the log-log representation represents the fractal dimension of the infinite pathway cluster, and is shown in the figure inset as a function of the chosen ΔV.

relaxation must be considerably slower and therefore not of importance for the MAE, in agreement with recent molecular dynamics simulations [27,28]. However, at high temperatures the time scale of the site relaxation will approach the inverse hopping rate of the alkali ions, and this makes it possible for an A ion to move to a previous B site and vice versa. This will reduce the efficiency of the blocking and thereby the MAE considerably, in accordance to experimental results. The experimental frequency dependence of the MAE can also be qualitatively understood since the decrease in the number of accessible sites for type A when these ions are substituted by B ions is less pronounced than the decrease in F (i.e., the local mobility of A ions is less affected than their long range mobility). Thereby it is obvious that our approach predicts a much lower MAE for high frequency experiments, where long range connectivity of the pathways is irrelevant.

Finally, one should note that although the blocking of pathways is by far the dominant contribution to the MAE a depression of the conductivity by nearly 1 order of magnitude would occur even if this contribution was ignored by not excluding the environments of B ions from the pathways of the A ions. The reason for this is that, e.g., the $Li_{0.5}Rb_{0.5}PO_3$ glass is due to its lower concentration of Li ions not as well adapted to Li cations as the $LiPO_3$ glass.

In conclusion, the approach to combine RMC modeling of mixed alkali phosphate glasses with the bond-valence method enables us to predict the MAE from the structural models of the glasses. The findings verify the assumptions made in the "random ion distribution model" [13] and show that the two types of alkali ions in a mixed alkali glass have distinctly different conduction pathways of low dimensionality, which means that A ions block the pathways for the B ions and vice versa. This blocking effect is the main reason for the experimentally observed MAE.

We thank C. Karlsson for providing us with conductivity data on the $Li_xRb_{1-x}PO_3$ glass system. J. S. is supported by a grant from the Knut and Alice Wallenberg Foundation. Financial support to J. S. from the Swedish Foundation for Strategic Research and to St. A. from the Deutsche Forschungsgemeinschaft is gratefully acknowledged.

[1] S. Chandra, *Superionic Solids, Principles and Applications* (North-Holland, Amsterdam, 1981).
[2] J. O. Isard, J. Non-Cryst. Solids **1**, 235 (1969).
[3] D. E. Day, J. Non-Cryst. Solids **21**, 343 (1976).
[4] M. D. Ingram, Phys. Chem. Glasses **28**, 215 (1987).
[5] R. L. McGreevy, Nucl. Instrum. Methods Phys. Res., Sect. A **354**, 1 (1995).
[6] R. L. McGreevy, J. Phys. Condens. Matter **13**, R877 (2001).
[7] I. D. Brown, *The Chemical Bond in Inorganic Chemistry-The Bond-Valence Model* (Oxford University Press, New York, 2002).
[8] I. D. Brown, Acta Crystallogr. Sect. B **53**, 381 (1997); **48**, 553 (1992).
[9] V. S. Urusov, Acta Crystallogr. Sect. B **51**, 641 (1995).
[10] G. P. Jr. Rouse *et al.*, J. Non-Cryst. Solids **28**, 193 (1978).
[11] A. C. Hannon *et al.*, J. Non-Cryst. Solids **150**, 97 (1992).
[12] J. Swenson *et al.*, Phys. Rev. B **58**, 11331 (1998).
[13] J. Swenson *et al.*, Phys. Rev. B **63**, 132202 (2001).
[14] B. Gee and H. Eckert, J. Phys. Chem. **100**, 3705 (1996).
[15] F. Ali *et al.*, Solid State NMR **5**, 133 (1995).
[16] T. Uchino *et al.*, J. Non-Cryst. Solids **146**, 26 (1992).
[17] S. Balasubramanian and K. J. Rao, J. Non-Cryst. Solids **181**, 157 (1995).
[18] J. Habasaki *et al.*, J. Non-Cryst. Solids **208**, 181 (1996).
[19] P. Maass *et al.*, Phys. Rev. Lett. **68**, 3064 (1992).
[20] P. Maass, J. Non-Cryst. Solids **255**, 35 (1999).
[21] G. N. Greaves and K. L. Ngai, Phys. Rev. B **52**, 6358 (1995).
[22] R. Kirchheim, J. Non-Cryst. Solids **272**, 85 (2000).
[23] St. Adams, Acta Crystallogr. Sect. B **57**, 278 (2001).
[24] St. Adams and J. Swenson, Phys. Rev. Lett. **84**, 4144 (2000); Phys. Rev. B **63**, 054201 (2000).
[25] St. Adams and J. Swenson, Phys. Chem. Chem. Phys. **4**, 3179 (2002).
[26] G. N. Greaves, J. Non-Cryst. Solids **71**, 203 (1985).
[27] P. Jund *et al.*, Phys. Rev. B **64**, 134303 (2001).
[28] J. Habasaki and H. Hiwatari, J. Non-Cryst. Solids **307**, 930 (2002).
[29] C. Karlsson *et al.*, Phys. Rev. B (to be published).